

Modelling of an Industrial Naphtha Isomerization Reactor and Development and Assessment of a New Isomerization Process

Ahmed M. Ahmed¹, Aysar T. Jarullah^{1,a}, Fayadh M. Abed², Iqbal M. Mujtaba^{3,a}

¹Tikrit University, College of Engineering, Chemical Engineering Department

²Tikrit University, College of Engineering, Mechanical Engineering Department

³Chemical Engineering Division, School of Engineering, University of Bradford,

Bradford BD7 1DP UK

^a Corresponding Author. *Email:* A.T.Jarullah@tu.edu.iq ; I.M.Mujtaba@bradford.ac.uk

Abstract

Naphtha isomerization is an important issue in petroleum industries and it has to be a simple and cost effective technology for producing clean fuel with high gasoline octane number. In this work, based on real industrial data, a detailed process model is developed for an existing naphtha isomerization reactor of Baiji North Refinery (BNR) of Iraq which involves estimation of the kinetic parameters of the reactor. The optimal values of the kinetic parameters are estimated via minimizing the sum of squared errors between the predicted and the experimental data of BNR. Finally, a new isomerization process (named as AJAM process) is proposed and using the reactor model developed earlier, the reactor condition is optimized which maximizes the yield and research octane number (RON) of the reactor.

Key words: Isomerization, Kinetic Parameters, Optimization, Mathematical Modeling

1. Introduction

Isomerization reactor is the heart of isomerization process (Figure 1) in petroleum refineries to enhance Research Octane Number (RON) of gasoline products. Isomerization is the rearrangement of straight-chain hydrocarbons components

converting to branched hydrocarbons components with higher octane number [1]. Contents of aromatics and olefins in the gasoline should be reduced for environmental protection and the loss of octane number caused by the reduction of aromatics and olefins should be compensated by addition of some compounds that have higher octane numbers. One possible alternative of aromatics and olefins is the branched alkanes with high octane numbers. Therefore, skeletal isomerization of alkanes is regarded a key reaction for producing environmentally benign gasoline in industries [2].

Reforming process is employed to produce high octane compounds, but this process is exclusively used for treating heavy naphtha (C7-C8). The isomerization process is regarded to be a simple, economic and very attractive solution to produce clean gasoline with a high octane number. Light naphtha is desirable to be included in gasoline formulation to meet the front-end distillation cut and octane number specs. The normal paraffins (C5/C6) is difficult to be included in the gasoline pool as it is because they have low octane number. Converting them to branched compounds with high octane number via isomerization process makes them more favorable for inclusion in gasoline [3,4].

Catalytic isomerization of pentanes and hexanes mixtures is usually conducted over a fixed bed of catalyst using hydrogen at operating conditions which minimizes the hydrocracking reactions but enhances the isomerization reactions. One or two reactors in series are used in such process, each one has an equal catalyst volume, and the reaction is acquired in the liquid or gas phase according to the catalyst used in the system [3,5].

The octane number of produced isomerizate is mainly dependent on the operation temperature of the reactor. Hydrocarbons isomerization reactions are reversible reactions and equilibrium conversion of n-paraffins increases with decreasing temperature (Figure 2). However, it is achieved after an infinite contact time of the feed in the reaction zone or at an equivalent very small value for liquid hourly space velocity. Such behavior is

represented in Figure 2 by theoretical conversion line (that neglects the effect of catalyst activity). In other words, for the actual behavior (represented in Figure 2 by actual conversion line), a decrease in temperature always corresponds to a decrease in reaction velocity due to decrease the effectiveness of the catalyst. Hence at low temperature, the actual conversion will be lower than the equilibrium conversion. On the other hand, as the isomerization reactions are exothermic, at high temperature (higher than the optimal temperature) the yield of iso-paraffins decreases with increasing temperature due to thermodynamic limitation [1,6].

In the traditional once through isomerization process (Figure 1), feedstock containing both iso-paraffins and normal paraffins are fed into the reactor where normal paraffins are converted to iso-paraffins to enhance the RON. The reaction products then pass through the stabilization unit and isomerizate is produced. Mathematical modeling of an industrial catalytic refining process is an important direction for technical improvement. Many studies in the past have greatly contributed to the improvement of the method of mathematical modeling for catalytic isomerization of light naphtha which is one of the most common high-tech industrial process [7,8].

This study aims to develop the process model of an industrial (BNR) isomerization reactor which requires development of kinetic models for the process. For this purpose, a full process model (taken from the literature) is used and the kinetic parameters (order of hydrocarbon concentration(n), order of hydrogen concentration in cracking reaction (m), order of hydrogen concentration in hydrogenation reaction (o), kinetic coefficient of intermolecular interactions intensity (α, γ), activation energies (E_j), pre-exponential factor (A_j)) of the model are estimated via minimizing sum of the squared error between the real industrial data (of BNR) and the model predictions to find the best kinetic parameters. Using the model, the reactor is then simulated by varying a number of operational

parameters. Finally, we have proposed a new isomerization process (named as AJAM process) configuration which is different from the existing BNR isomerization process. We have evaluated this proposed process by comparing its performance (in terms of yield and RON) with the existing BNR process. The validated isomerization reactor model developed earlier is employed in the new process.

2. Industrial Reactor Operation

All the industrial data including the reactor dimensions, catalyst specifications, reactor's feedstock, product's composition and operating conditions, which are presented in Tables 1, 2, and 3 are taken from the actual isomerization unit at Baiji North Refinery (BNR), Iraq. Isomerization unit of BNR operates in once through mode using zeolitic catalyst system. As illustrated in Figure 1, the fresh feedstock (light naphtha) obtained from hydrotreating process is fed to the unit feed storage drum and then mixed with compressed hydrogen before being heated in heat exchangers and furnace system, which raises the temperature of the feed to the optimal reactor inlet temperature. Thereafter, the light naphtha passes through the isomerization reactor only once where the n-paraffins are converted to iso-paraffins.

The isomerization reactions take place in the reactor (cylindrical with a height of 13.840 m and diameter of 2.9 m) loaded with a bed of zeolite catalyst. Unstabilized isomerizate is sent to stabilization unit in order to separate light hydrocarbons (mainly CH_4 , C_2H_6 and C_3H_8 which used to produce LPG). The stabilized isomerizate is taken out from the bottom of the column as a final product.

3. Mathematical model of BNR isomerization reactor

The model equations of isomerization reactor are represented by a system of equations of material balance and heat balance for each component as shown below:

3.1 Mass balance equation

Eq. (1) is an ordinary differential equation used to describe the concentration of every component through the catalyst bed. However, solution of this differential equation gives the concentration profile of components with unit volume of catalyst bed [9].

$$G \frac{dC_i}{dV} = \sum_{j=1}^m a_j \cdot r_j \quad (1)$$

The initial conditions of this equation are:

$$\text{At } V=0, \quad C_i = C_{i,in}$$

3.2. Heat Balance Equation

Solution of the following ordinary differential Eq. (2) gives the temperature profile over the unit volume of the catalyst bed [9].

$$G \frac{dT}{dV} = \frac{1}{\rho C_p^m} \sum_{j=1}^m Q_j \cdot a_j \cdot r_j \quad (2)$$

The initial conditions can be written as:

$$\text{At } V=0, \quad T=T_{in}$$

3.3. Reaction Rate Equations

According to the chemical reaction, power rate law non-elementary reaction rate at the set temperature is proportional to the concentration of reacting substances based on the order of n, m and o as shown below [9]:

$$r_j = \eta_j k_j C_i^n \quad (3)$$

$$r_j = \Omega_j k_j C_i^n C_{H_2}^o \quad (4)$$

$$r_j = \Omega_j k_j C_i^n C_{H_2}^m \quad (5)$$

Eq. (3, 4 and 5) represents the isomerization, hydrogenation and hydrocracking reactions rate respectively.

Reaction rate constant (k_j) can be described by Arrhenius equation as follow:

$$k_j = A_j \exp\left(\frac{-E_j}{R T}\right) \quad (6)$$

The concentration of each component can be described by the ideal gas law with taken into account the compressibility factor:

$$C_i = (y_i p)/(Z_i R T) \quad (7)$$

The compressibility factor for every species is given by the following equation [10]:

$$Z_i = 1 - \frac{(T/T_{ci})}{(P/P_{ci})\left(0.36748758 - \frac{0.04188423(T/T_{ci})}{(P/P_{ci})}\right)} \quad (8)$$

Based on the operating data of different isomerization process, **Chekantsev et al.** [9] have proposed a scheme of the isomerization reactions process presented in Figure 3, which is employed in the modeling of naphtha isomerization process according to the chemical reaction equations presented in Table 1.

3.4. Catalyst Activity

The dependence of catalyst activity on time has been taken in to account that can be represented by the following equation [9]:

$$a = \frac{k_{j,current}}{k_{j,initial}} \quad (9)$$

3.5. Effectiveness Factor

The effectiveness factor of reactions represents the ratio of the reaction rate into the particle to the rate of reaction at the surface of the particle as submit by **Bischoff** [11] and **Mohammed et al.** [12] and can be estimated as a function of Thiele Modulus valid for cylindrical particle as follow:

$$\eta_j = \frac{\tanh\varphi_j}{\varphi_j} \quad (10)$$

For n^{th} -order reaction, the general Thiele Modulus (φ) can be evaluated using the following relationship [12,13]:

$$\varphi = \frac{V_P}{S_P} \sqrt{\left(\frac{n+1}{2}\right) \left(\frac{r_j C_i^{-1} \rho_p}{D_{e,i}}\right)} \quad (11)$$

The Particle density (ρ_p), is estimated using the following relation [14]:

$$\rho_p = \frac{\rho_{cat}}{1-\epsilon_B} \quad (12)$$

The Bed porosity (ϵ_B) of the catalyst can be estimated for undiluted sphere packed catalyst from the following equation [12]:

$$\epsilon_B = 0.38 + 0.073 \left(1 + \frac{\left(\frac{d_t}{d_{pe}} - 2\right)^2}{\left(\frac{d_t}{d_{pe}}\right)^2} \right) \quad (13)$$

Equivalent diameter of particle (d_{pe}) can be defined as the diameter of the sphere having the same external volume as the real catalyst particle [15,16].

$$d_{pe} = \frac{6(V_p/S_p)}{\phi_s} \quad (14)$$

$$\phi_s = \frac{\text{surface area of a sphere of equal volume}}{\text{surface area of the particle}} \quad (15)$$

For cylindrical shape, the external volume (V_p) and the surface area (S_p) of particle is calculated as shown below:

$$V_p = \frac{\pi}{4} d_p^2 L \quad (16)$$

$$S_p = \pi d_p L \quad (17)$$

The effective diffusivity of every component ($D_{e,i}$) can be estimated utilizing the next relation [12] taking into account the tortuosity of the pore network inside the catalyst particle considering the porosity in the modeling.

$$D_{e,i} = \frac{\epsilon_s}{\tau} \frac{1}{\frac{1}{D_{mi}^g} + \frac{1}{D_{ki}}} \quad (18)$$

Catalyst particle porosity (ϵ_s) is calculated by using the equation below, which depends on the particle density and pore volume:

$$\epsilon_s = \rho_p V_g \quad (19)$$

The tortuosity factor (τ) can be estimated by the following equation [13].

$$\tau = \frac{1-0.5 \log \epsilon_s}{\epsilon_s} \quad (20)$$

Knudsen diffusivity represents the diffusivity of components into pores of the catalyst for each component, which can be calculated utilizing the following equation [12]:

$$D_{ki} = 349200 r_g \sqrt{\frac{T}{MW_i}} \quad (21)$$

The mean pore radius can be calculated by the following equation [12].

$$r_g = \frac{2V_g}{S_g} \quad (22)$$

The molecular diffusivity coefficient of species i in the gas phase can be calculated from equation (23) depending on the binary diffusion coefficient of component i through the other components [17]

$$D_{mi}^g = (1 - y_i) / \sum_{k \neq i}^{NCG} \frac{y_k}{D_{i,k}} \quad (23)$$

The binary diffusion coefficient can be calculated from the following equation [18].

$$D_{i,k} = 188.2458 * 10^{-20} \sqrt{T^3 \left(\frac{1}{MW_i} + \frac{1}{MW_k} \right)} \frac{1}{P \sigma_{i,k}^2 \Omega_D} \quad (24)$$

The average collision diameter and the collision diameter of each component is calculated by the equation below [19]:

$$\sigma_{i,k} = \frac{\sigma_i + \sigma_k}{2} \quad (25)$$

$$\sigma_i = 1.18 * 10^{-9} (V_{bi})^{\frac{1}{3}} \quad (26)$$

The diffusion collision integral for gases molecules can be calculated using the equation below [20].

$$\Omega_D = \frac{1.06036}{(T^*)^{0.1561}} + \frac{0.193}{\exp(0.47635T^*)} + \frac{1.03587}{\exp(0.01529T^*)} + \frac{1.76474}{\exp(3.89411T^*)} \quad (27)$$

The dimensionless temperature is calculated as a function of Boltzmann constant (C_B) and Characteristic (minimum) energy (ε_{ik}) [19].

$$T^* = \frac{T}{\varepsilon_{ik}/C_B} \quad (28)$$

$$\varepsilon_{ik}/C_B = 0.75T_{c,ik} \quad (29)$$

$$T_{c,ik} = \sqrt{T_{ci}T_{ck}} \quad (30)$$

3.6 Density of Mixture

The density of mixture (ρ) represents the light naphtha vapor density (ρ_{ln}) and hydrogen gas density (ρ_{H2}) as follow:

$$\rho = \rho_{ln}Wt_{ln} + \rho_{H2}Wt_{H2} \quad (31)$$

The density of light naphtha is estimated as a function of pure components density and their weight fractions as follow:

$$\rho_{ln} = \sum_i \rho_i Wt_i \quad (32)$$

Where, ρ_i : Density of i hydrocarbon component vapor, kg/m^3 , Wt_i : Weight fraction of i hydrocarbon component, (-).

The density of hydrogen and of each hydrocarbon component in the gas phase can be estimated as a function of temperature and pressure based on ideal gas equation with taking into account the gas compressibility factor where the gas at these conditions has trend toward the reality state. The equation can be written as shows:

$$\rho_i = \frac{PMW_i}{Z_iRT} \quad (33)$$

Where:

P : Pressure, p_a

T : Temperature, K

Z_i : The gas compressibility factor, (-)

R : Gas constant, $J/mol. K$

MW_i : Molecular weight of i^{th} component, $kg/kmol$

The density of the components at normal boiling point can be calculated from the following equation [18]:

$$\rho_{bi} = \frac{MW_i P_{ci}}{R T_{ci} Z_{ci} (1 + (1 - T_{ri})^{2/7})} \quad (34)$$

Where:

ρ_b : The density at boiling point, kg/m^3

Z_c : Critical compressibility factor, (-)

T_r : Reduced temperature, (-)

P_c : Critical pressure, p_a

T_c : Critical temperature, K

$$T_r = \frac{T}{T_c} \quad (35)$$

3.7 Heat of Reaction Calculation

The heat of reaction as a function of temperature is calculated from the following equations:

$$Q_j = \Delta H_{rxn,j}^\circ + \int_{298}^T \Delta C p_j dT \quad (36)$$

$$\Delta H_{rxn,j}^\circ = \sum y_i \Delta H_{fi,p}^\circ - \sum y_i \Delta H_{fi,r}^\circ \quad (37)$$

$$\Delta Cp_j = \sum y_i Cp_{i,p} - \sum y_i Cp_{i,r} \quad (38)$$

$$Cp_i = A + BT + CT^2 + DT^3 \quad (39)$$

The heat capacity of mixture (Cp_m) can be calculated from following equation:

$$Cp_m = \sum y_i Cp_i \quad (40)$$

3.8 Flow Rate of Raw Material

The feed stock to the reactor contains hydrogen gas and light naphtha vapor that can be calculated as a function to the mass flow rate of light naphtha (W_{ln}) and hydrogen (W_{H_2}) as follow:

$$G = W_{ln}/\rho_{ln} + W_{H_2}/\rho_{H_2} \quad (41)$$

The mass flow rate of light naphtha is calculated as a function to LHSV and the volume of the bed (V):

$$W_{ln} = Q_{ln} * sp. gr * \rho_w \quad (42)$$

$$Q_{ln} = LHSV * V \quad (43)$$

$$W_{H_2} = m_r * M_{ln} * MW_{H_2} \quad (44)$$

$$M_{ln} = \frac{W_{ln}}{MW_{ln}} \quad (45)$$

$$MW_{ln} = \sum_i y_i MW_i \quad (46)$$

3.9 Research Octane Number (RON) and yield

The model has taken into account the physicochemical nature of mixing process and non-additive properties of gasoline. Thus, the model of mixing octane number can be written as [21]:

$$RON = \sum_{i=1}^m (RON_i \cdot y_i) + \beta \quad (47)$$

$$\beta = \frac{1}{100} \sum_{i=1}^{m-1} \sum_{j=2}^m \beta_i \beta_j y_i y_j \quad (48)$$

$$\beta_i = \alpha \left(\frac{Di_i}{Di_{max}} \right)^\gamma \quad (49)$$

$$Yield = M_{iso}/M_{In} \quad (50)$$

4. Estimation of kinetic parameters of the reactor model

Accurate estimations for kinetic parameters are required to describe the actual behavior of process. However, parameter estimation is a difficult step in the development of process models and requires experimental data. Thus, the best evaluation of such parameters is based on minimum errors between the experimental (industrial) data and the predicted data from the mathematical model [16].

The optimal kinetic parameters of an industrial light naphtha isomerization reactor model are estimated using gPROMS software. The optimal values of activation energy (E_j) and pre-exponential factor (A_j), components concentration orders (o, m & n) and kinetic coefficient of intermolecular interactions intensity (γ & α) for every reaction in the process were directly calculated by using non-linear approach. Also, such parameters were simultaneously calculated in this approach based on minimization of the sum of the squared error (SSE) between experimental and predicted weight fraction, yield and RON.

$$SSE = \sum \left(\sum_{i=1}^m ((W_i^{exp.} - W_i^{pred.})^2 + (yield^{exp.} - yield^{pred.})^2 + (RON^{exp.} - RON^{pred.})^2) \right) \quad (51)$$

4.1 Optimization problem formulation for parameter estimation

The optimization problem formulation of naphtha isomerization process can be described as follows:

- Give:** The reactor configuration, the initial hydrocarbons and hydrogen concentration, the catalyst, reaction temperature and pressure, liquid hourly space velocity and flow rate.
- Obtain:** The reaction orders of hydrocarbon (n), hydrogen (m , o), pre-exponential constant (A_j), activation energy (E_j) of each reaction and also kinetic coefficients (α & γ).
- So as to minimize:** The sum of square errors (SSE).
- Subjected to:** Constraints of process and linear bounds upon all optimization variables in this process.

Mathematically, the optimization problem can be represents as shown below:

$$\begin{aligned}
 &\text{Min} && SSE \\
 &\text{s.t.} && f(v, (v), \tilde{x}(v), u(v), z) = 0, [v_0, v_f] && \text{(model, equality constraint)} \\
 &&& n^L \leq n \leq n^U && \text{(Inequality constraints)} \\
 &&& m^L \leq m \leq m^U && \text{(Inequality constraints)} \\
 &&& o^L \leq o \leq o^U && \text{(Inequality constraints)} \\
 &&& E_j^L \leq E_j \leq E_j^U && \text{(Inequality constraints)} \\
 &&& A_j^L \leq A_j \leq A_j^U && \text{(Inequality constraints)} \\
 &&& \alpha_j^L \leq \alpha_j \leq \alpha_j^U && \text{(Inequality constraints)} \\
 &&& Y_j^L \leq Y_j \leq Y_j^U && \text{(Inequality constraints)}
 \end{aligned}$$

Where: $f(v, x(v), \tilde{x}(v), u(v), \underline{v}) = 0$: represents the model of process which presented in the previous sections. V : the reactor bed volume. $U(v)$: the decision variables ($n, m, E_j, A_j, \alpha, Y$). $X(v)$: gives the set of all algebraic and differential variables (C_i, T, R, \dots).

$\tilde{x}(v)$: represents the differential variables derivative with respect to volume of the reactor bed such as $(\frac{dC_i}{dv}, \frac{dT}{dv}, \dots)$. \underline{V} : volume (independent constants parameters) or variables of design such as $(R \dots)$. $[v_0, v_f]$: the volume interval of interest. The function f is supposed to be continuously differentiable with regard to whole its arguments.

The optimization solution method used by gPROMS is a two-step method known as feasible path approach. The first step performs the simulation to converge all the equality constraints (described by f) and to satisfy the inequality constraints. The second step performs the optimization (updates the values of the decision variables such as the kinetic parameters). The optimization problem is posed as a Non-Linear Programming (NLP) problem and is solved using a Successive Quadratic Programming (SQP) method within gPROMS software.

4.2 The kinetic model of the industrial reactor

All the catalyst specifications, inlet and outlet composition of the industrial isomerization reactor, operating condition of the industrial isomerization reactor and the physical properties of light naphtha components are given in Tables (2 - 5). The critical properties and molecular weight of each component were taken from **Perry and Green** [22], pure components RON were taken from **Chekantsev et al.** [9] and dipole moment values were taken from **Vogel and Mobius** [23]. The lower and upper bounds for all listed inequality constraints in addition to the initial values of the applied model are presented in appendix A (Table A1).

The optimal values of activation energy (E_j) and pre-exponential factor (A_j) for every reaction in the process have been calculated using Arrhenius equation. Also, the optimal values of components concentration orders (α , m & n) and kinetic coefficient of

intermolecular interactions intensity (γ & α) were simultaneously estimated. Such parameters are presented in Tables 6 and 7.

The optimal kinetic parameters have been estimated based on a maximum error of 0.1% among all results between the experimental and predicted results of average reactor output data of three test runs. The composition of isomerizate components (W_i), research octane number of isomerizate (RON) and reactor outlet temperature (T) are obtained via simulation process and presented in Table 8.

As can be seen from this Table, the error between the industrial data and predicted results is very small giving a clear indication that the results obtained have an excellent match among theoretical and practical results. Therefore, the model can now be applied confidently for further applications for the purpose of improving the yield and RON of such process. Many researchers have studied the kinetics of isomerization of light naphtha, as reported in literatures [9,24,25]. They have assumed that the concentration orders used in the simulation of isomerization process equal to the number of molecules, which enter the reaction. Thus, huge errors (more than 5%) between the industrial and theoretical results were reported in the past giving high deviation.

5. Simulation of Industrial Reactor

After getting the accurate kinetic model, the parameters are used to describe the influence of operating conditions on the reactions occurring through the bed of catalyst. Increasing the RON of the light naphtha and isomerizate yield are the main goal of the isomerization process. Therefore, the variables are considered as an index for analyzing the performance of the reactor.

5.1 Effect of Temperature and Pressure on the isomerizate RON and yield

Figures 4 and 5 show the influence of the feed stock temperature and pressure on the RON and yield of isomerizate respectively. Feed stock no.1 was used to describe the behavior of this process at constant LHSV equal to 1.489 hr^{-1} and hydrogen ratio equal to 3.22.

It can be observed that temperature has the most impact on the performance of the isomerization reactions. In Figure 4, at the beginning of the curve (region one 512-534K), the RON decreases with increasing temperature, which can be related to the thermodynamic properties of such reactions and accelerated the hydrocracking of hydrocarbons containing six carbon atoms such as 2,2-DMB, 2,3-DMB, MCP, and CH. Therefore, the high octane number species are converted to lighter ones such as methane, propane and butanes. These light species are separated from the product in the form of fuel gas and the reduction of octane number continues until hydrocarbon species containing six carbons are hydrocracked. Finally, the upward trend of RON in the second region is due to increase the percentage of pentane at higher temperatures [26].

Since hydrocracking reactions have a negative effect on the yield of the gasoline production, it is concluded that the optimal isomerization temperature is located in the first region in which RON and yield are both at the optimal values. This Figure also indicates that 0.2 MPa increment in pressure leads to increase the optimal temperature about 2°C . Figure 5 demonstrates the dependency of RON on pressure when hydrogen to hydrocarbon molar ratio and LHSV are kept constant. The optimal reactor inlet temperature depends on the pressure and the results showed that by decreasing the reactor pressure. The reactor inlet temperature should be reduced until the desired temperature inside the reactor is achieved for the purpose of reducing the hydrocracking reactions, which absorbs some of isomerization reactions emitted heat [1, 27].

Figure 5 presents the effect of inlet feed stock temperature and pressure on the isomerizate yield at constant LHSV and hydrogen to hydrocarbon mole ratio. The results show that the yield of isomerizate decreases with increasing inlet temperature leading to enhancement of hydrocracking reactions rate. Also, this Figure shows that the increase in pressure can decrease the isomerizate yield due to increase in the partial pressure of hydrogen [23,26].

5.2 Effect of Hydrogen to Hydrocarbon Mole Ratio on the isomerizate RON and yield

Hydrogen is desired to complete the reactions and to reduce the deposition of coke on the surface of the catalyst. Figures 6 - 8 show the influence of the hydrogen to hydrocarbons mole ratio on the RON and Figure 9 - 11 illustrate the impact of hydrogen to hydrocarbons mole ratio on the yield of isomerizate at constant temperature, pressure and liquid hourly space velocity. It has been observed from Figure 6, 7 and 8 that the product RON depends on the hydrogen over feed molar ratio. These results show that at constant feed flow rate and by increasing hydrogen to feed molar ratio, the RON of product decreases due to increase the rate of hydrocracking reactions (which considered endothermic reactions) within the reactor [23, 26].

Figures 9 - 11 demonstrate the high negative impact of hydrogen to hydrocarbon mole ratio on the isomerizate yield. Increasing of such ratio leads to decrease in the yield of isomerizate owing to the increase of hydrogen partial pressure. This Figure also indicates that 0.2 unit increments in hydrogen-to-hydrocarbon molar ratio decreases the yield of isomerizate about 1.3% at constant temperature.

5.3 Effect of LHSV on the isomerizate RON and yield

Figures 12 - 14 present the effect of LHSV on the RON and Figures 15 - 17 illustrate the influence of LHSV on the yield of isomerizate at constant H₂/HC mole ratio, temperature and pressure. According to Figure 8, the RON of the product depends on the LHSV. Indeed, the residence time decreases by increasing the LHSV, so that the conversion of normal paraffin's decrease [27].

The negative effect of increasing the LHSV on the RON can be overcome by increasing the inlet temperature of reactor feed stock. This method can be recommended for increasing the capacity of light naphtha isomerization reactor, accordingly, increasing the reactor operating temperature increases the capacity of gasoline production while the RON of product remains at the desired value. This procedure is highly appreciated when there is limitation in increasing hydrogen to hydrocarbon molar ratio due to the process limitations such as the loading capacity of hydrogen compressor [23].

6. A new isomerization process configuration

Figure 18 shows the new proposed configuration of the isomerization process. Compared to the traditional process (BNR) shown in Figure 1, the new configuration separates the normal paraffins from the isomerizate. Only normal paraffins are allowed to go into the isomerization reactor. The process is expected to maximize the yield and RON of the isomerizate. In all other traditional isomerization technologies, the adsorption equipment are located after the reactor to separate the normal paraffins and recycling them to the reactor. Such processes results in increase in the isomerization feed stock leading to increase in the equipment capacity. In the new configuration, based on the specifications of naphtha feed stock at BNR isomerization unit, the separation process can take place first (adsorption equipment located before the reactor) to reduce the benzene percentage less than 0.62%, so that it is not hydrogenated through isomerization process (benzene

components are left the adsorber with branched paraffins). Also, this procedure reduces the reactor feed stock by 46% in comparison with once through process.

As can be seen in Figure 18, the naphtha feed stock enters to the adsorption column where the normal paraffins are adsorbed by the molecular sieve then desorbed by hydrogen stream and the stream of normal paraffins and the hydrogen are sent to the reactor to produce the branched chain paraffins. The reactor outlet stream is a mixture of normal and iso-paraffins, so it is combined with the naphtha feed stock stream to separate the normal paraffins through adsorption process. The benefits expected of using such new configuration is increased RON of the isomerizate unit and reduced isomerization reactor feed stock, increased yield in comparison with the traditional once through process. Also this procedure will reduce the isomerization reactor capacity compared to the once through process. Due to the separation and by-pass operation made for iso-paraffins, the yield of isomerizate will increase owing to reduction of the hydrocracking reactions.

6.1 Modeling of the proposed isomerization process

The reactor model presented in section 3 with the optimal kinetic parameters (calculated in section 4) is used to represent the isomerization reactor of the new configuration (Figure 18) and is incorporated in an optimization framework to maximize (RON and yield) of the reactor, taken into account the change of feed stock rate and inlet composition of component due to separation of normal paraffins upfront. The performance of the reactor is optimized according to Eq. (52) below:

$$OBJ = \Sigma(RON + YIELD) \quad (52)$$

Given Initial concentration, kinetic parameters, reactor configuration, process specifications.

Determine Initial temperature, pressure, LHSV and hydrogen to hydrocarbon mole ratio.

So as to maximize OBJ (RON & yield).

Subject to Process constraints and linear bounds on all decision variables.

The optimization problem is stated as:

Max OBJ

P, T, LHSV, m_r , W_{nC_5} , W_{nC_6}

s.t $f(x(z), u(z), v) = 0$ (model equation, equality constraint)

$$P^L \leq P \leq P^U \quad (\text{inequality constraints})$$

$$T^L \leq T \leq T^U \quad (\text{inequality constraints})$$

$$LHSV^L \leq LHSV \leq LHSV^U \quad (\text{inequality constraints})$$

$$m_r^L \leq m_r \leq m_r^U \quad (\text{inequality constraints})$$

$$W_{nC_5}^L \leq W_{nC_5} \leq W_{nC_5}^U \quad (\text{inequality constraints})$$

$$W_{nC_6}^L \leq W_{nC_6} \leq W_{nC_6}^U \quad (\text{inequality constraints})$$

6.2 Performance of the new isomerization process and comparison with the BNR isomerization process

The optimal results obtained for the new process configuration (Figure 18) (that has not previously been reported in the literature) and the comparison with the current once through BNR process (Figure 2), are presented in Table 9. As clearly noted, the highest RON and yield is obtained by using the new process compared with those obtained by traditional method. Increase in RON from 79.45 to 90.81 is due to increase in the total conversion of normal paraffins. While, increase in the yield from 97.68 to 99.2 is due to decrease in the reactor feed stock rate by 48.34 wt% compared to once through process.

Also, the bed volume (V) of the proposed new process has been decreased by 46.5% in comparison with once through process.

7. Conclusions

In this work, an isomerization reactor model of a traditional once through process (Figure 1) is developed using industrial data of Baiji North Refinery (BNR). The parameters of the kinetic models have been determined by using model based parameter estimation technique. The model is then used to simulate the industrial reactor and to study the effect of different operating parameters such as temperature, pressure, H₂/HC mole ratio and LHSV on the performance of the reactor in terms of RON and the yield. Finally, a new isomerization process configuration (Figure 18) is proposed and its performance is evaluated and compared with the traditional process. For this purpose, the reactor model developed earlier is used to optimize the reactor conditions giving the maximum RON and isomerizate yield. The new process outperforms the traditional process in terms of reactor feed rate and reactor bed volume has been decreased by 46% (at the same unit feed rate for both) compared with once through process.

Often, in the literature a process model is developed based on lab scale experimental process which is then used to evaluate large scale process by incorporating conditions for scale-up. However, in this work the model is developed based on real large scale industrial data which shows the novelty of this work and then the model is used to develop and assess a new (which is again novel) isomerization process.

Finally note, if someone wants to use the model developed in this work for small scale process, they have to change the flow rate and the size of the catalyst used to get the same trends observed in this study.

Abbreviations

Symbols	Definitions
2,2-DMB	2,2-Dimethyl butane
2,3-DMB	2,2-Dimethyl butane
2-MP	2-methyl pentane
3-MP	3-methyl pentane
ACP	Advanced configuration process
B	Benzene
C ₅	Pentane components
C ₆	Hexane components
CH	Cyclo hexane
CP	Cyclo pentane
H ₂	Hydrogen
HC	Hydrocarbons
i-C ₄	Iso-butane
i-C ₇	Iso-heptane
i-P	Iso-pentane
n-C ₄	Normal butane
n-C ₇	Normal heptane
n-P	Normal pentane
n-H	normal hexane
Pt	platinum
Wt%	weight fraction

Nomenclature

Symbol	Description	Unit
a	Catalyst activity	(-)
A	Pre-exponential factor	$(mol/m^3)^{1-n}hr^{-1}$
B	is a total deviation of hydrocarbons octane number from additively	(-)
C_B	Boltzmann constant	(-)
C_{H_2}	Hydrogen concentration	mol/m^3
C_i	Concentration of i^{th} component	mol/m^3
$C_{i,in}$	Initial (inlet) concentration of i^{th} component	mol/m^3
C_p	The heat capacity of streams	$kJ/(kg. ^\circ C)$
$C_{p,i,p}$	Heat capacity of reaction product components	$J/mol.K$
$C_{p,i,r}$	Heat capacity of reaction reactant components	$J/mol.K$
$C_{p,m}$	Heat capacity of mixture	$J/(kg. k)$
C_{p,H_2}	The specific heat capacity at constant pressure	$J/(kg. k)$
d_{pe}	Equivalent particle diameter	m
D_e	Effective diffusivity	m^2/hr
$D_{i,k}$	Binary diffusion coefficient of i^{th} component through the other components	m^2/hr
Dk_i	Knudsen diffusivity coefficient of species i in the gas phase	m^2/hr
D_{mi}^g	Molecular diffusivity coefficient of species i in the gas phase	m^2/hr
D_r	Reactor diameter	
Di_i	Dipole moment of molecule i	Debye
Di_{max}	Maximum possible dipole moment of the	Debye

	hydrocarbons mixture	
E	Activation energy	$J/mol.K$
G	raw material flow rate	m^3/hr^{-1}
i	hydrocarbon components number	(-)
j	Reaction number	(-)
k	Apparent reaction rate constant	$(mol/m^3)^{1-n}hr^{-1}$
L	Particle length	m
$LHSV$	Liquid hourly space velocity	hr^{-1}
m	Order of hydrocarbons concentration in dehydrogenation reaction	(-)
m_r	Mole ratio of hydrogen to light naphtha	(-)
M	Total moles interred the reactor	mol
$M_{iso.}$	Moles of isomerizate	mol
M_{H2}	Total moles interred the reactor	mol
M_{ln}	Moles of naphtha feed	mol
MW_i	Molecular weight of hydrocarbon i	$kg/kmol$
MW_{H2}	Molecular weight of hydrogen	$kg/kmol$
MW_{ln}	Molecular weight of light naphtha	$kg/kmol$
n	Order of hydrocarbons concentration	(-)
o	Order of hydrocarbons concentration in hydrogenation reaction	(-)
P	Reactor pressure	Pa
q_j	Heat of j^{th} reaction	kJ/mol
q_p	power of ith pump	kJ/hr

r_g	Mean pore radius,	m
R	Gas constant	$J/mol.K$
RON	Research octane number	(-)
RON_i	i^{th} pure component research octane number	(-)
S_g	Specific surface area of particle	m^2/kg
S_p	Total geometric surface area	m^2
$sp.gr$	Specific gravity	(-)
T^*	Dimensionless temperature	(-)
y	Mole fraction	(-)
Z	Compressibility factor	(-)

Greek Letter

η	Effectiveness factor	(-)
ϕ	Thiel Modulus	(-)
P_{ln}	Liquid (naphtha) density	kg/m^3
P_{H2}	Vapor (hydrogen) density	kg/m^3
ρ_p	Particle density	kg/m^3
ρ_{bi}	Liquid density of component i at normal boiling Point	kg/m^3
ϵ_B	Bed porosity	(-)
Φ_s	Shape factor	(-)
ϵ_s	Catalyst particle porosity	(-)
$\sigma_{i,k}$	Average collision diameter	m
\mathcal{I}_D	Collision integral for diffusion	(-)
σ_i	Collision diameter of i^{th}	m
σ_k	Collision diameter of k^{th} components	m

$\varepsilon_{l,k}$	Characteristic (minimum) energy	K
$\Delta\dot{H}_{rxn,j}$	Standard heat of jth reaction	<i>kJ/mol</i>
ΔCp_j	Heat capacity of j th reaction	<i>kJ/mol.K</i>
$\Delta\dot{H}_{fi,p}^{\circ}$	Standard heat of formation of reaction product components	<i>kJ/mol</i>
$\Delta\dot{H}_{fi,r}^{\circ}$	Standard heat of formation of reaction reactant components	<i>kJ/mol.K</i>
y	Mole fraction	(-)
β_i, β_k	Parameters showing the tendency of i th molecule to intermolecular interaction with k th molecule	(-)
γ, α	Kinetic coefficients defining the intensity of intermolecular interactions from dipole moment	(-)
err	Error function	(-)
τ	Tortuosity factor	

References

- [1] E.A. Yasakova, A.V. Sitdikova, A.F. Achmetov, Tendency of Isomerization Process Development in Russia and Foreign Countries, *Oil and Gas Business*, 1 (2010) 1-7.
- [2] M.J. Moran, J.S. Zogorski, P.J. Squillace, MTBE and gasoline hydrocarbons in ground water of the United States *Ground water*, 43 (2005) 615-627.
- [3] S. Parkash, *Refining processes handbook*, Gulf Professional Publishing, United States of America, 2003.
- [4] C.I. Koncsag, I.A. Tutun, C. Safta, Study of C5/C6 isomerization on Pt/H-zeolite catalyst in industrial conditions, *Ovidius University Annal. Chem.* 22 (2011) 102-106.

- [5] C.H. Bartholomew, R.J. Farrauto, Fundamentals of industrial catalytic processes, John Wiley & Sons. Iselin, New Jersey, (2011).
- [6] G. Anderson, R. Rosin, M. Stine, M. Hunter, New solutions for light paraffin isomerization, NPRA Annual Meeting, Washington DC, AM-04-46, (2004).
- [7] P.S. Barcia, J.A. Silva, A.R.E. Rodrigues, Adsorption dynamics of C5/C6 isomerase fractions in zeolite beta for the octane improvement of gasoline, Energy & Fuels, 24 (2010) 1931-1940.
- [8] K.Watanabe, T.Kawakami, K.Baba, N. Oshio, T. Kimura, Simultaneous isomerization and desulfurization of sulfur-containing light naphtha over metal/SO₄²⁻/ZrO₂-Al₂O₃ catalyst, Applied Catalysis A: General, 276 (2004) 145-153.
- [9] N.V. Chekantsev, M.S. Gyngazova, E.D. Ivanchina, Mathematical modeling of light naphtha (C5, C6) isomerization process, Chemical Engineering Journal, 238 (2014) 120-128.
- [10] T.H. Ahmed, Hydrocarbon phase behavior, Gulf Pub Co. Houston, (1989).
- [11] K.B. Bischoff, Effectiveness factors for general reaction rate forms, American Institute of Chemical Engineers Journal, 11 (1965) 351-355.
- [12] A.E. Mohammed, A.T. Jarullah, S.A. Ghani, I.M. Mujtaba, Optimal design and operation of an industrial three phase reactor for the oxidation of phenol, Computers & Chemical Engineering, 94 (2016) 257-271.
- [13] G.F. Froment, K.B. Bischoff, Chemical reactor analysis and design, Wiley, New York, (1979).
- [14] M.O. Tarhan, Catalytic reactor design, McGraw-Hill Companies, (1983).
- [15] B. Cooper, B. Donnison, B. Moyse, Hydroprocessing conditions affect catalyst shape selection, Oil Gas J. 84 (1986) 49.

- [16] A.T. Jarullah, Kinetic modeling simulation and optimal operation of trickle bed reactor for hydrotreating of crude oil, Ph.D. Thesis, University of Bradford, (2011).
- [17] C. Wilke, P. Chang, Correlation of diffusion coefficients in dilute solutions, American Institute of Chemical Engineers Journal, 1 (1955) 264-270.
- [18] H.G. Rackett, Equation of state for saturated liquids, Journal of Chemical and Engineering Data, 15 (1970) 514-517.
- [19] R.B. Bird, J.O. Hirschfelder, C.F. Curtiss, Molecular theory of gases and liquids, John Wiley, (1954).
- [20] P.D. Neufeld, A. Janzen, R. Aziz, Empirical Equations to Calculate 16 of the Transport Collision Integrals^{(l, s)*} for the Lennard/Jones (12-6) Potential, The Journal of Chemical Physics, 57 (1972) 1100-1102.
- [21] M.S. Gyngazova, A.V. Kravtsov, E.D. Ivanchina, M.V. Korolenko, N.V. Chekantsev, Reactor modeling and simulation of moving-bed catalytic reforming process, Chemical Engineering Journal, 176 (2011) 134-143.
- [22] R.H. Perry, D.W. Green, Perry's chemical engineers' handbook, McGraw-Hill Professional (1999).
- [23] V. Vogel, D. Mabijs, Local surface potentials and electric dipole moments of lipid monolayers: contributions of the water/lipid and the lipid/air interfaces, Journal of colloid and interface science, 126 (1988) 408-420.
- [24] M. Busto, J. Grau, S. Canavese, C. Vera, Simultaneous hydroconversion of n-hexane and benzene over Pt/WO₃/ZrO₂ in the presence of sulfur impurities, Energy & Fuels, 23 (2008) 599-606.
- [25] G.S. Volkova, S.I. Reshetnikov, L.N. Shkuratova, A.A. Budneva E.A. Paukshtis, n-Hexane skeletal isomerization over sulfated zirconia catalysts with different Lewis acidity, Chemical Engineering Journal, 134 (2007) 106-110.

- [26] R. Hayati, S.Z. Abghari, S. Sadighi, M. Bayat, Development of a rule to maximize the research octane number (RON) of the isomerization product from light naphtha, Korean Journal of Chemical Engineering, 32 (2015) 629-635.
- [27] M.M. Said, T.S. Ahmed, T.M. Moustafa, Predictive Modeling and Optimization for an Industrial Penex Isomerization Unit: A Case Study, Energy & Fuels 28 (2014) 7726-7741.

List of Tables

Table 1: Chemical reactions equations for isomerization processes

Table 2: Catalyst specifications

Table 3: Inlet and outlet composition of isomerization reactor through test run days

Table 4: Operating condition of isomerization reactor through test run days

Table 5: Values of physical properties of light naphtha components used in the model

Table 6: Optimal values of pre-exponential factor and activation energy of every reaction

Table 7: Optimal orders of components concentration and kinetic coefficient of intermolecular interactions intensity

Table 8: The comparison between the experimental data and the mathematical model results (predicted)

Table 9: Comparison between the performance and operating conditions of once through (conventional method) and proposed process

Table A1: Lower and upper bounds for all listed inequality constraints of the applied model

Table A2: Initial values for all listed inequality constraints of the applied model

List of Figures

Figure 1: Block diagram of once through process (BNR process)

Figure 2: Effect of temperature on the conversion of n-paraffins [1]

Figure 3: Scheme of formalized reaction for isomerization process

Figure 4: Effect of temperature on the RON of product at different pressure with constant LHSV of 1.489 hr^{-1} and H_2/HC at 3.22 mole ratio

Figure 5: Yield of isomerizate at different temperature and pressure and at constant LHSV of 1.489 hr^{-1} and H_2/HC at 3.22 mole ratio

Figure 6: Effect of H₂/HC on the RON at constant temperature equal to 523K, LHSV at 1.489 hr⁻¹ and pressure of 2.4MPa

Figure 7: Effect of H₂/HC on the RON at constant temperature of 523K, LHSV of 1.489 hr⁻¹ and pressure at 2.4MPa

Figure 8: Effect of H₂/HC on the RON at constant temperature of 526K, LHSV of 1.489 hr⁻¹ and pressure at 2.4MPa

Figure 9: Yield of isomerizate at constant temperature of 520K, LHSV of 1.489 hr⁻¹ and pressure of 2.4MPa

Figure 10: Yield of isomerizate at constant temperature of 523K, LHSV of 1.489 hr⁻¹ and pressure of 2.4MPa

Figure 11: Yield of isomerizate at constant temperature of 526K, LHSV of 1.489 hr⁻¹ and pressure of 2.4MPa

Figure 12: Effect of LHSV on RON at constant temperature of 520K, H₂/HC at 3.22 and pressure of 2.4 MPa

Figure 13: Effect of LHSV on RON at constant temperature of 523K, H₂/HC at 3.22 and pressure of 2.4 MPa

Figure 14: Effect of LHSV on RON at constant temperature of 526K, H₂/HC at 3.22 and pressure of 2.4 MPa

Figure 15: Effect of LHSV on yield at constant temperature of 520K, H₂/HC of 3.236 and pressure of 2.4MPa

Figure 16: Effect of LHSV on yield at constant temperature of 523K, H₂/HC of 3.236 and pressure of 2.4MPa

Figure 17: Effect of LHSV on yield at constant temperature of 526K, H₂/HC of 3.236 and pressure of 2.4MPa

Figure 18: Block diagram of the proposed new isomerization process (named as AJAM process) in this study

Table 1: Chemical reactions equations for isomerization processes

Reaction NO. (j)	Chemical reaction equations	Reaction NO. (j)	Chemical reaction equations
1	$n-C_5H_{12} \xrightarrow{\text{yields}} i-C_5H_{12}$	19	$n-C_4H_{10} + H_2 \xrightarrow{\text{yields}} Gas$
2	$i-C_5H_{12} \xrightarrow{\text{yields}} n-C_5H_{12}$	20	$i-C_4H_{10} + H_2 \xrightarrow{\text{yields}} Gas$
3	$n-C_6H_{14} \xrightarrow{\text{yields}} 2-MP$	21	$n-C_5H_{12} + H_2 \xrightarrow{\text{yields}} Gas$
4	$2-MP \xrightarrow{\text{yields}} n-C_6H_{14}$	22	$i-C_5H_{12} + H_2 \xrightarrow{\text{yields}} Gas$
5	$n-C_6H_{14} \xrightarrow{\text{yields}} 3-MP$	23	$n-C_6H_{14} + H_2 \xrightarrow{\text{yields}} Gas$
6	$3-MP \xrightarrow{\text{yields}} n-C_6H_{14}$	24	$2-MP + H_2 \xrightarrow{\text{yields}} Gas$
7	$2,3 - DMB \xrightarrow{\text{yields}} 2-MP$	25	$3-MP + H_2 \xrightarrow{\text{yields}} Gas$
8	$2-MP \xrightarrow{\text{yields}} 2,3 - DMB$	26	$2,3-DMB \xrightarrow{\text{yields}} Gas$
9	$2,3DMB \xrightarrow{\text{yields}} 2,2 - DMB$	27	$2,2-DMB \xrightarrow{\text{yields}} Gas$
10	$2,2DMB \xrightarrow{\text{yields}} 2,3 - DMB$	28	$n-C_7H_{16} + H_2 \xrightarrow{\text{yields}} Gas$
11	$n-C_7H_{16} \xrightarrow{\text{yields}} i-C_7H_{16}$	29	$i-C_7H_{16} + H_2 \xrightarrow{\text{yields}} Gas$
12	$i-C_7H_{16} \xrightarrow{\text{yields}} n-C_7H_{16}$	30	$CH + H_2 \xrightarrow{\text{yields}} n-C_6H_{14}$
13	$MCP \xrightarrow{\text{yields}} CH$	31	$MCP + H_2 \xrightarrow{\text{yields}} 2-MP$
14	$CH \xrightarrow{\text{yields}} MCP$	32	$MCP + H_2 \xrightarrow{\text{yields}} 3-MP$
15	$3 - MP \xrightarrow{\text{yields}} 2-MP$	33	$MCP + H_2 \xrightarrow{\text{yields}} 2,2-DMB$
16	$2 - MP \xrightarrow{\text{yields}} 3-MP$	34	$MCP + H_2 \xrightarrow{\text{yields}} 2,3-DMB$
17	$c-C_5H_{12} + H_2 \xrightarrow{\text{yields}} n-C_5H_{12}$	35	$B + 3H_2 \xrightarrow{\text{yields}} CH$
18	$c-C_5H_{12} + H_2 \xrightarrow{\text{yields}} i-C_5H_{12}$	36	$B + 3H_2 \xrightarrow{\text{yields}} MCP$

Table 2: Catalyst specifications

Parameter	Symbol	Unit	Value
Catalyst bed length	L	m	11.24
Catalyst bed diameter	D_r	m	2.9
Catalyst bulk density	ρ_{cat}	kg/m^3	741
length of catalyst particle	l_p	m	3.5×10^{-3}
Diameter of catalyst particle	d_p	m	1.8×10^{-3}
Specific volume of particle	V_g	m^3/kg	0.4
Specific surface area of particle	S_g	m^2/kg	450

Table 3: Inlet and outlet composition of isomerization reactor through test run days

Hydrocarbon components	Test run 1		Test run 2		Test run 3		Average	
	inlet	outlet	inlet	outlet	inlet	outlet	input	outlet
n-Butane (nC4)	2.821	1.222	4.253	1.970	3.549	1.963	3.479	1.855
n-Pentane(nC5)	23.954	18.267	25.977	18.362	26.59	17.423	25.81	18.39
n-Hexane(nC6)	17.338	7.540	14.320	7.597	15.09	8.169	15.95	7.343
n-Heptane (nC7)	1.221	0.040	2.816	0.059	1.401	0.032	1.314	0.051
i-Butane (iC4)	0.216	0.517	0.353	0.963	0.259	0.735	0.287	0.950
i-pentane (iC5)	17.775	35.013	20.652	35.689	22.00	35.982	20.11	36.07
2,2 Di Methyl Butane (2,2DMB)	0.622	7.766	0.451	7.356	0.581	7.170	0.548	7.293
2,3 Di Methyl Butane (2,3DMB)	2.180	3.567	1.472	3.092	1.748	3.029	1.911	3.390
2 Methyl Pentane (2MP)	12.314	12.493	9.311	12.597	9.736	12.978	10.26	12.561
3 Methyl Pentane (3MP)	9.996	9.296	7.294	8.599	7.946	8.243	8.401	8.404
i-heptane (iC7)	3.764	0.412	5.084	0.250	3.483	0.298	3.556	0.273
Cyclo Pentane (CP)	1.529	1.138	1.312	1.369	1.175	1.054	1.174	1.054
Methyl Cyclo Pentane (MCP)	2.973	1.450	2.574	1.072	3.078	1.144	2.873	1.144
Cyclo Hexane (CH)	1.137	0.436	1.270	0.316	1.101	0.353	1.240	0.353
Benzene (C6)	0.496	0.000	0.433	0.000	0.498	0.004	0.470	0.000

Table 4: Operating condition of isomerization reactor through test run days

	Liquid hourly space velocity (hr^{-1})	Temperature (K)	Pressure (MP)	Hydrogen make-up ($\text{kg}_{\text{H}_2}/\text{kg}_{\text{HC}}$)
First day	1.489	523.12	2.340	3.324
Second day	1.561	525.72	2.472	3.227
Third day	1.622	526.2	2.430	3.381
average	1.557	524.14	2.414	3.310

Table 5: Values of physical properties of light naphtha components used in the model

Components	Molecular Weight (kmol/kg)	Critical temperature (K)	Critical Pressure (Mpa)	Critical compressibility Factor, (-)	Dipole Moment (depy)	Research octane number
Normal butane	58.123	425.16	3.7963	0.2791	0.127	95
Iso-butane	58.123	407.85	3.6397	0.2780	0.132	100.2
Normal pentane	72.125	471.10	3.3550	0.2747	0.114	62
Iso-pentane	72.125	469.70	3.3812	0.2611	0.121	92
Cyclo-pentane	70.135	511.60	4.5057	0.2871	0.241	102.3
Normal hexane	86.177	488.71	3.0068	0.2642	0.080	24
2-methyl pentane	86.177	497.50	3.0096	0.2669	0.097	74.4
3-methyl pentane	86.177	504.50	3.1240	0.2732	0.099	75.5
2,3-dimethyl butane	86.177	500.21	3.8163	0.3284	0.121	105
2,2-dimethyl butane	86.177	488.71	3.0816	0.2704	0.124	95
Cyclo-hexane	84.162	553.40	4.0710	0.2791	0.320	84
Normal heptane	100.25	540.206	2.7358	0.2624	0.0	0
Iso-heptane	100.25	530.30	2.7397	0.2597	0.0	84
Methyl cyclopentane	84.162	531.70	3.7845	0.2724	0.0	96
Benzene	78.114	562.16	4.8953	0.2713	0.0	120
Hydrogen	2.0160	33.200	1.3000	0.3050	(-)	(-)

Table 6: Optimal values of pre-exponential factor and activation energy of every reaction

Reaction number (j)	Activation energy (E_j), J/mol	Pre-exponential factor (A_j)	Reaction number (j)	Activation energy (E_j), J/mol	Pre-exponential factor (A_j)
1	10359.1	30328.2	19	410171	1.20053E+37
2	10359.1	11973.8	20	382917	1.11887E+37
3	1779.64	8101.04	21	329776	6.71002E+31
4	1779.64	12237.8	22	342906	2.04715E+31
5	3098.58	34360	23	266712	6.27716E+26
6	3098.58	6149	24	264004	3.04961E+26
7	12499.3	36715.9	25	294374	6.36194E+26
8	12499.3	7720	26	277806	1.70425E+27
9	8551.55	8549.55	27	273965	6.77152E+26
10	8551.55	2516.07	28	220534	3.17332E+23
11	12410.4	246504	29	216658	3.51283E+23
12	12410.4	11903	30	128748	1.74229E+15
13	5888	4326.49	31	91332.9	283811864
14	5888	4610.34	32	98599.4	15238268830
15	7703	102328	33	97396.6	9654847240
16	7703	2806.19	34	91034.3	1400727929
17	185323	1.20775E+16	35	259025	2.92353E+29
18	180018	3.98326E+16	36	255393	2.90342E+26

Table 7: Optimal orders of components concentration and kinetic coefficient
of intermolecular interactions intensity

Parameter	Symbol	Unit	Value
Order of hydrocarbon concentration	n	(-)	0.9412
Order of hydrogen concentration in cracking reaction	m	(-)	0.9350
Order of hydrogen concentration in hydrogenation reaction	o	(-)	3.279
Kinetic coefficient of intermolecular interactions intensity	α	(-)	1.463
	γ	(-)	0.8154

Table 8: The comparison between the experimental data and the mathematical model results (predicted)

Hydrocarbon components	Test run 1			Test run 2			Test run 3		
	Exp.	Theo.	Absolute Error (%)	Exp.	Theo.	Absolute Error (%)	Exp.	Theo.	Absolute Error (%)
n-Butane(nC4)	1.222	1.2208	0.0982	1.970	1.9681	0.0964	1.963	1.9611	0.0968
n-Pentane(nC5)	18.267	18.248	0.101	18.362	18.179	0.101	17.423	17.250	0.101
n-Hexane(nC6)	7.540	7.5329	0.094	7.597	7.5893	0.094	8.169	8.1606	0.094
n-Heptane(nC7)	0.040	0.4004	0.100	0.059	0.0591	0.1094	0.032	0.3203	0.0938
i-Butane(iC4)	0.517	0.5165	0.0967	0.963	0.9621	0.0934	0.735	0.7343	0.0953
i-pentane(iC5)	35.013	34.977	0.1028	35.689	35.653	0.1008	35.982	35.946	0.1005
2,2 Di Methyl Butane (2,2-DMB)	7.766	7.7589	0.0914	7.356	7.3487	0.0992	7.170	7.1629	0.0990
2,3 Di Methyl Butane (2,3-DMB)	3.567	3.5635	0.0981	3.092	3.0889	0.1002	3.029	3.0259	0.1023
2Methyl Pentane (2MP)	12.493	12.469	0.1001	12.597	12.472	0.1001	12.978	12.965	0.1001
3Methyl Pentane (3MP)	9.296	9.2867	0.1002	8.599	8.5903	0.1015	8.243	8.2345	0.1009
i-heptane (iC7)	0.412	0.4116	0.0990	0.250	0.2498	0.0992	0.298	0.2977	0.0979
Cyclo Pentane (CP)	1.138	1.1391	0.1007	1.369	1.3703	0.0981	1.054	1.0551	0.0998
Methyl Cyclo Pentane (MCP)	1.450	1.4488	0.0832	1.072	1.0712	0.0786	1.144	1.1431	0.0720
Cyclo Hexane (CH)	0.436	0.4356	0.0910	0.316	0.3157	0.0879	0.353	0.3527	0.0728
Benzene (C6)	2.87E-6	2.89E-6	0.6969	2.76E-6	2.78E-6	0.7246	2.83E-6	2.84E-6	0.3536
Temperature (T)	552.12	551.34	0.1012	550.72	551.67	0.097	554.2	553.4	0.1006
RON	79.33	79.374	0.0554	79.41	79.452	0.0528	79.26	79.317	0.0719

Table 9: Comparison between the performance and operating conditions of once through (conventional method) and proposed process

Variables	Unit	Value	
		Once Through Process (Figure 1)	Proposed Process (Figure 18)
RON	(-)	79.452	90.81
Yield	(%)	97.6831	99.20
Unit feed rate	Ton/hr	75.841	75.841
Reactor feed rate	Ton/hr	75.841	40.96
Isomerizate rate	Ton/hr	74.083	75.234
Bed volume (V)	m ³	74.20	39.74
T	K	524.314	521.09
P	MPa	2.406	2.104
LHSV	hr ⁻¹	1.507	1.503
m_r	(-)	3.31	3.46

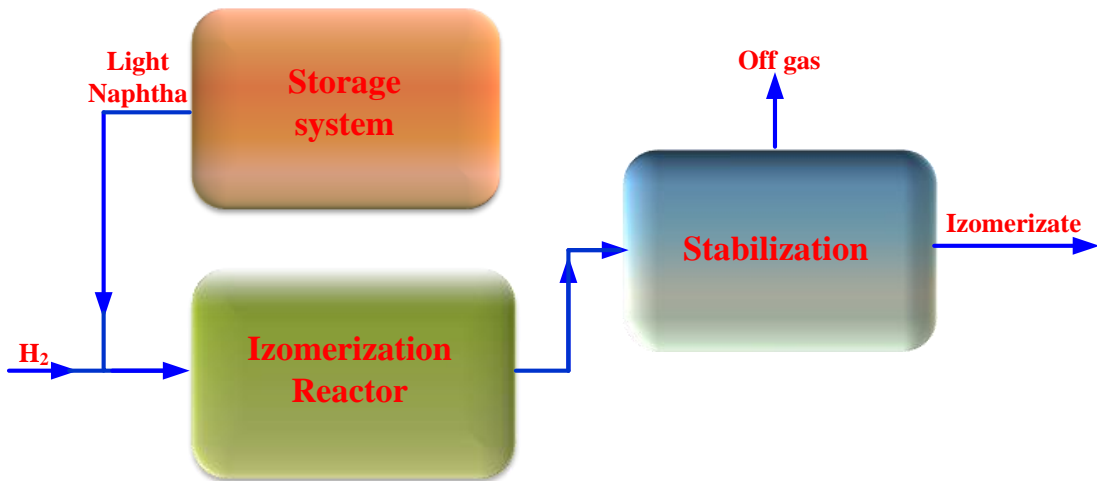


Figure 1: Block diagram of once through process (BNR process)

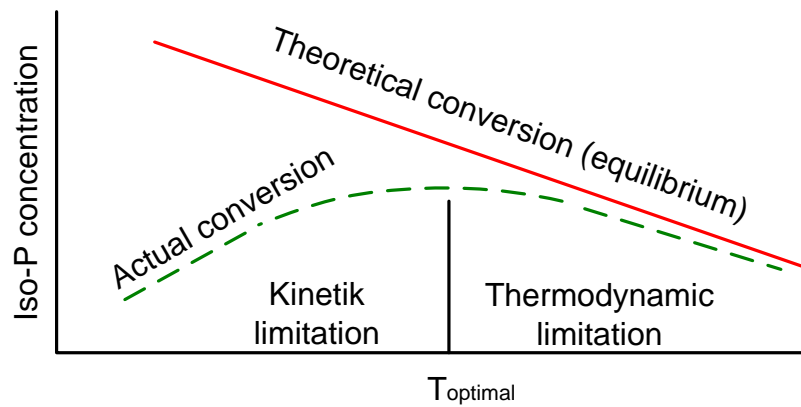


Figure 2: Effect of temperature on the conversion of n-paraffins [1]

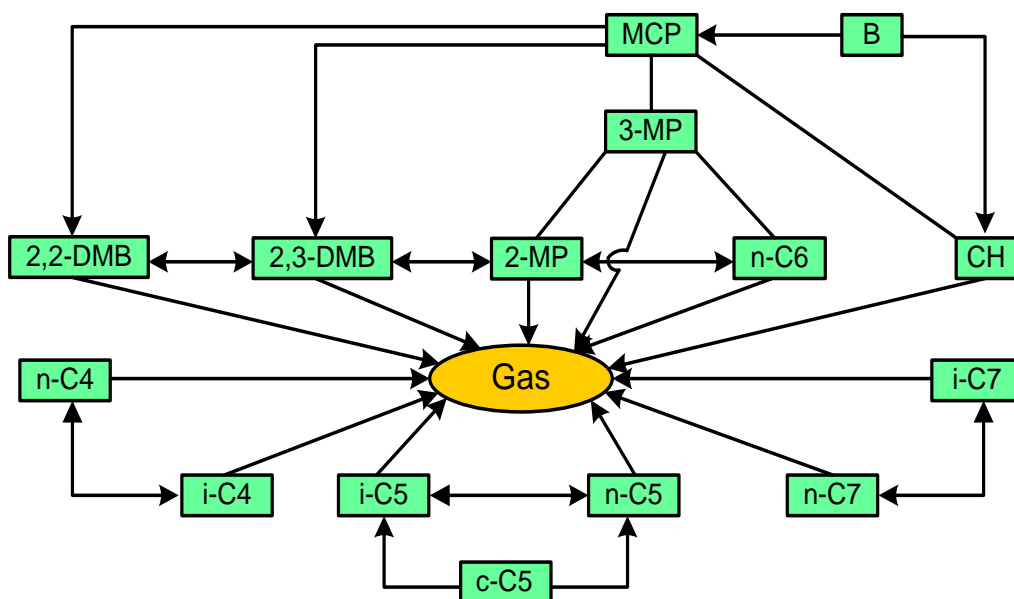


Figure 3: Scheme of formalized reaction for isomerization process

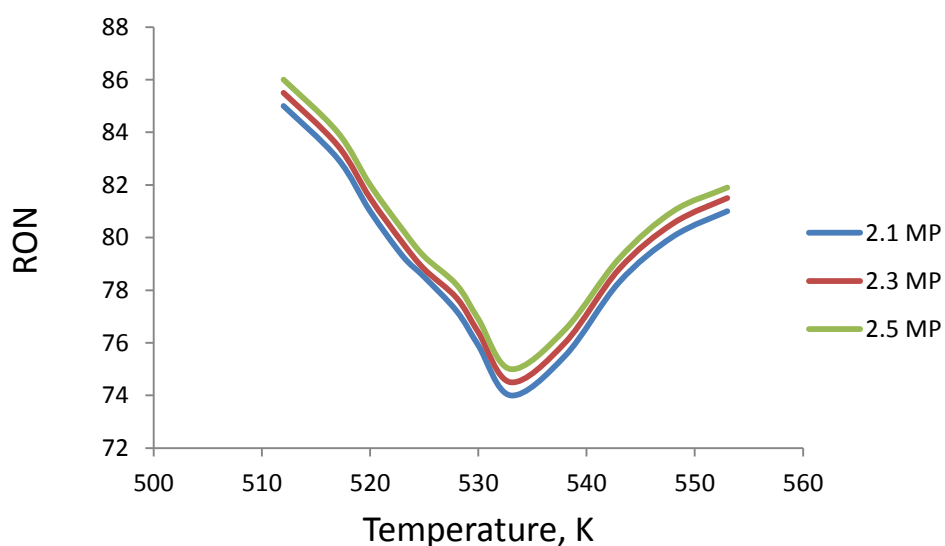


Figure 4: Effect of temperature on the RON of product at different pressure with constant LHSV of 1.489 hr^{-1} and H_2/HC at 3.22 mole ratio

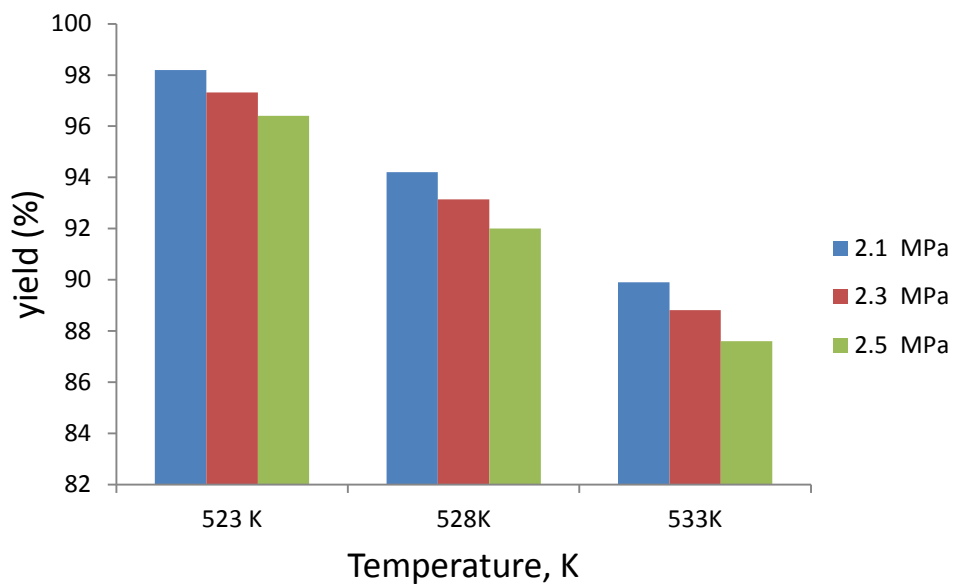


Figure 5: Yield of isomerizate at different temperature and pressure and at constant LHSV of 1.489 hr^{-1} and H_2/HC at 3.22 mole ratio

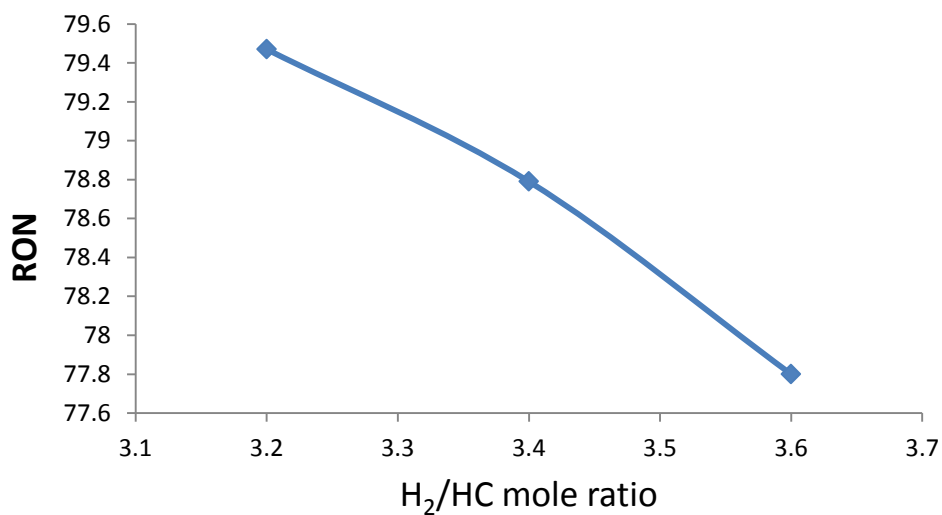


Figure 6: Effect of H_2/HC on the RON at constant temperature equal to 523K, LHSV at 1.489 hr^{-1} and pressure of 2.4MPa

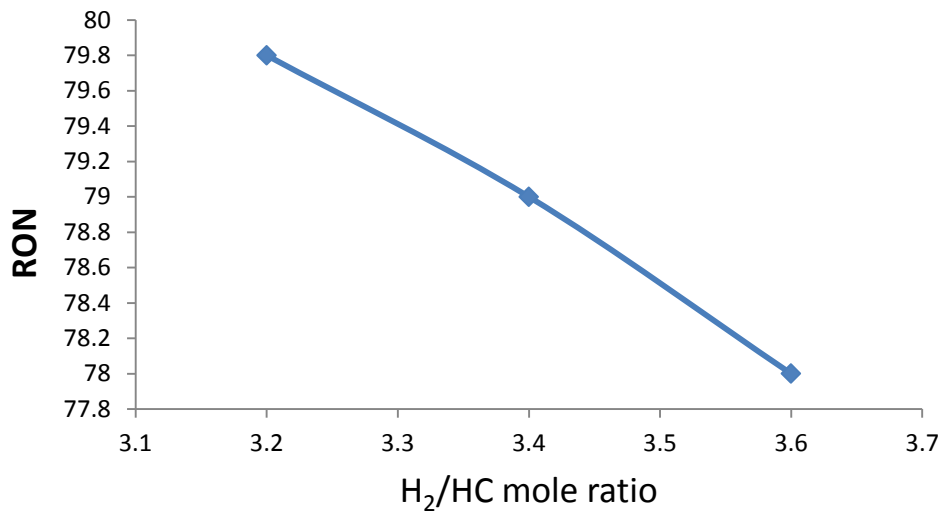


Figure 7: Effect of H₂/HC on the RON at constant temperature of 523K, LHSV of 1.489 hr⁻¹ and pressure at 2.4MPa

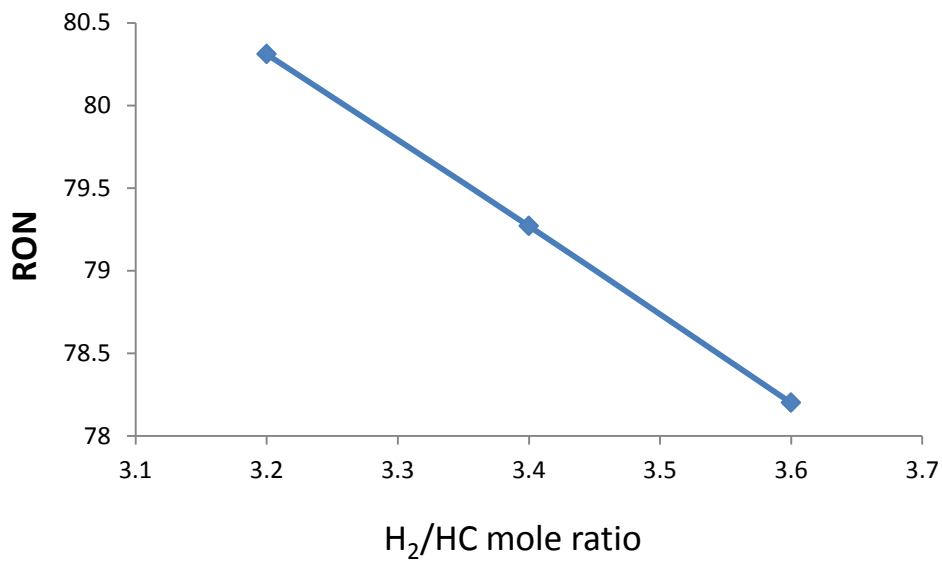


Figure 8: Effect of H₂/HC on the RON at constant temperature of 526K, LHSV of 1.489 hr⁻¹ and pressure at 2.4MPa

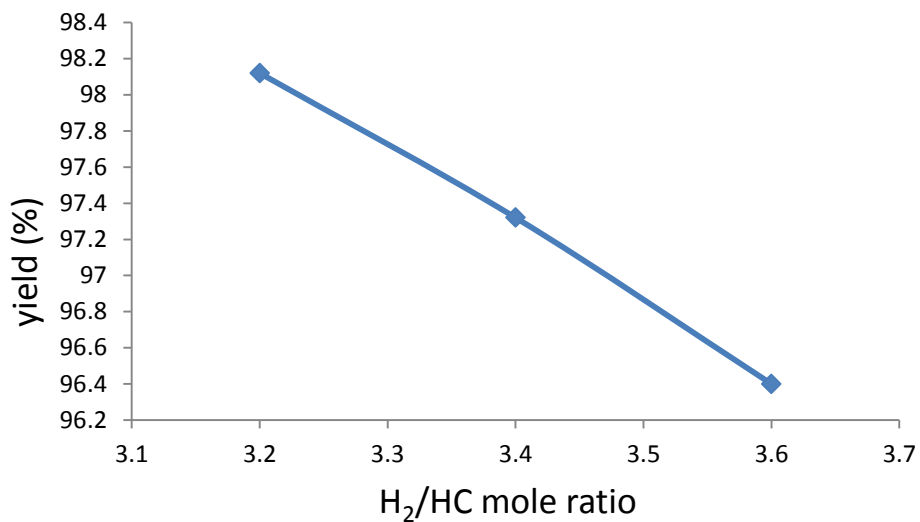


Figure 9: Yield of isomerizate at constant temperature of 520K, LHSV of 1.489 hr⁻¹ and pressure of 2.4MPa

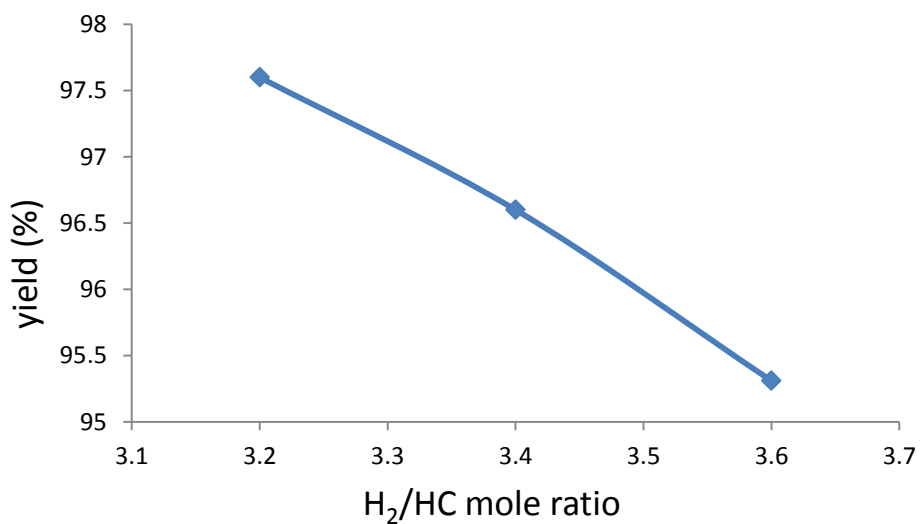


Figure 10: Yield of isomerizate at constant temperature of 523K, LHSV of 1.489 hr⁻¹ and pressure of 2.4MPa

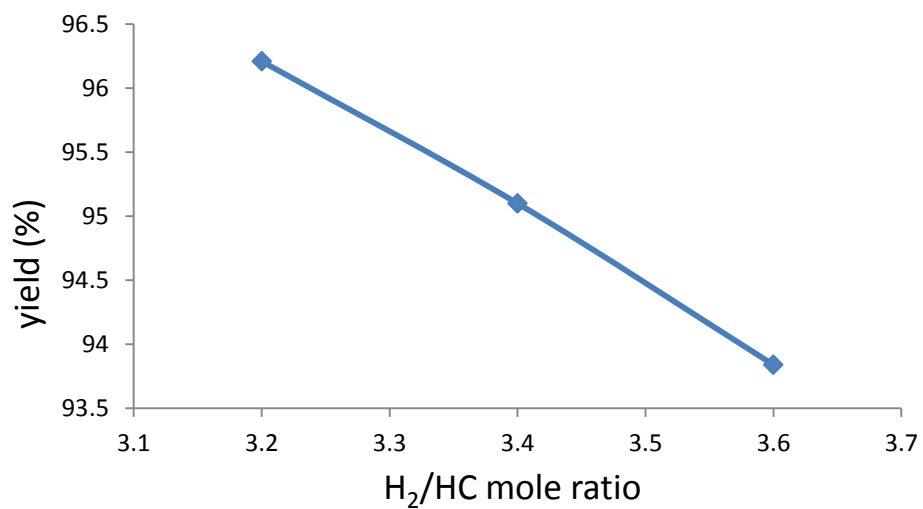


Figure 11: Yield of isomerizate at constant temperature of 526K, LHSV of 1.489 hr⁻¹ and pressure of 2.4MPa

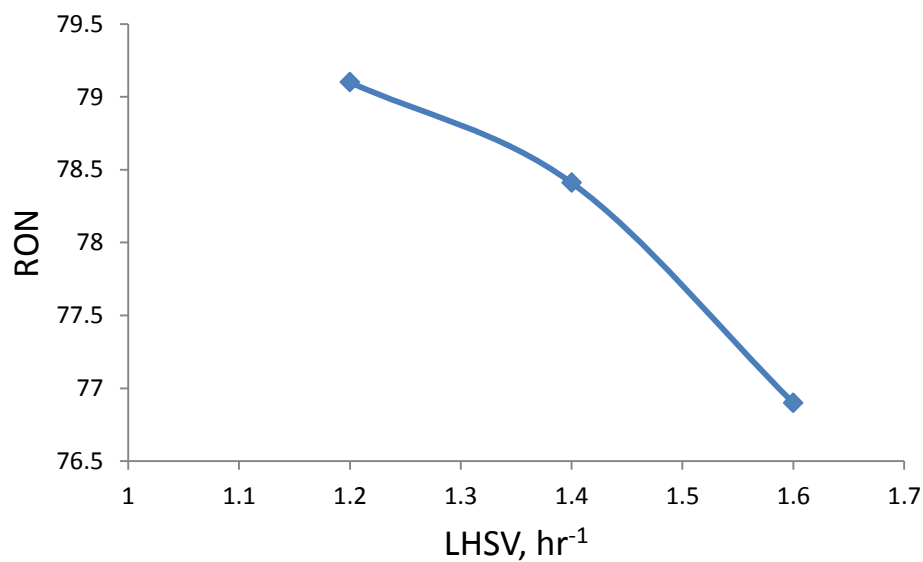


Figure 12: Effect of LHSV on RON at constant temperature of 520K, H₂/HC at 3.22 and pressure of 2.4 MPa

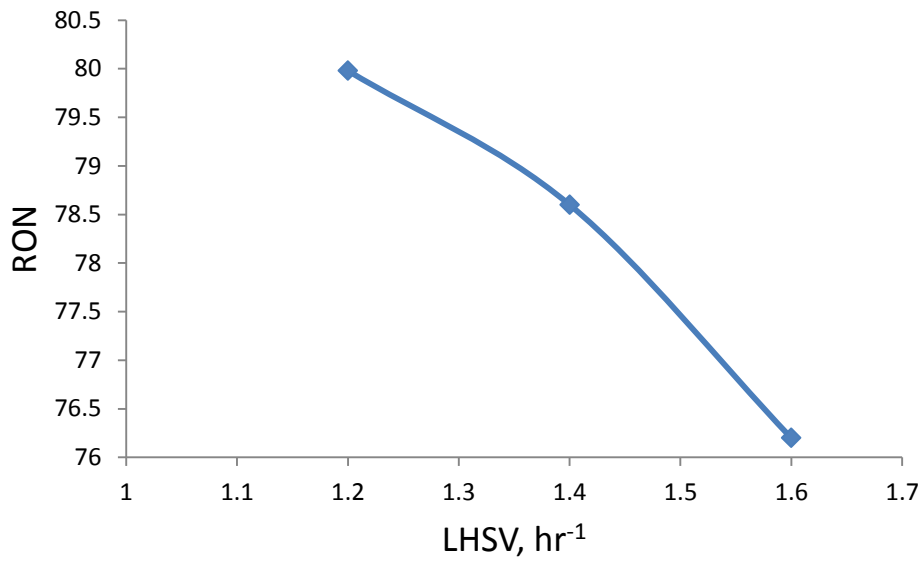


Figure 13: Effect of LHSV on RON at constant temperature of 523K, H₂/HC at 3.22 and pressure of 2.4 MPa

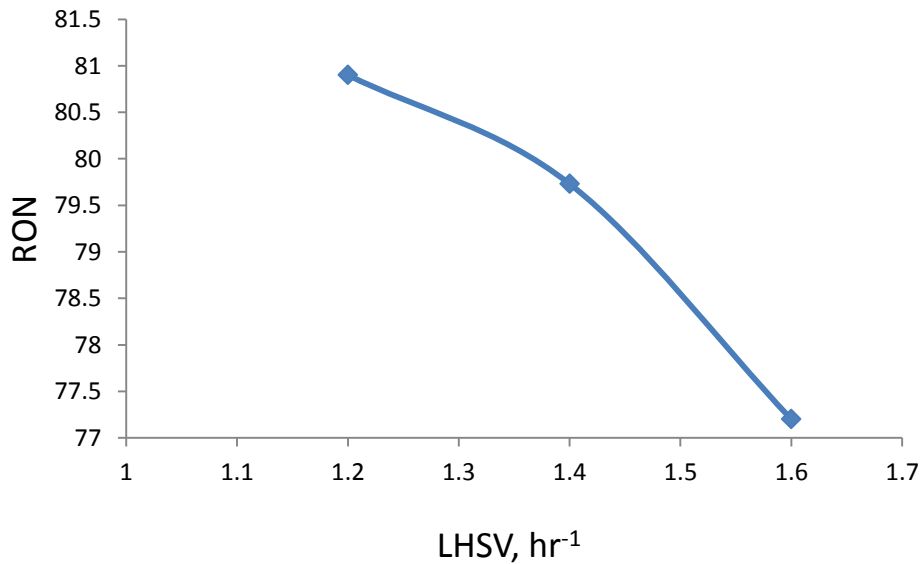


Figure 14: Effect of LHSV on RON at constant temperature of 526K, H₂/HC at 3.22 and pressure of 2.4 MPa

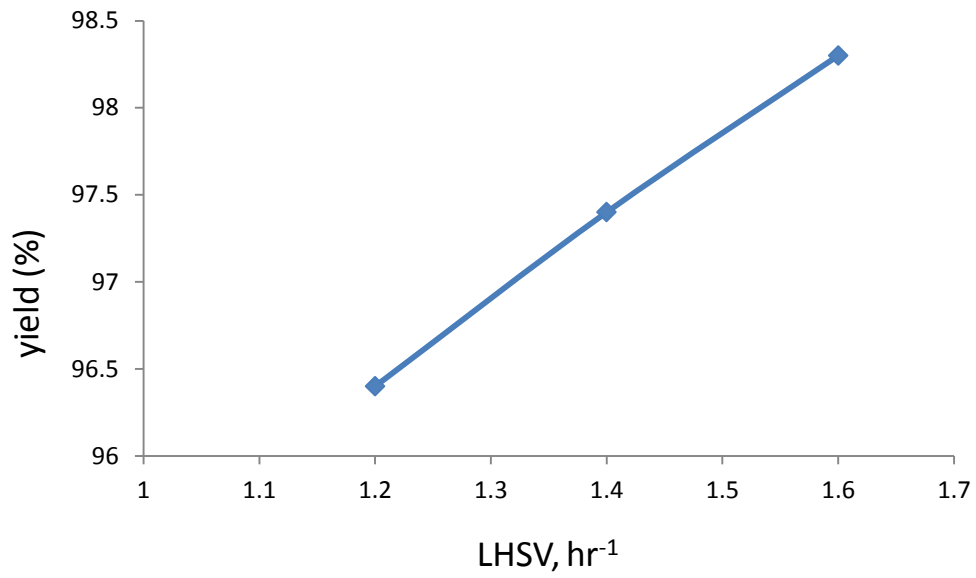


Figure 15: Effect of LHSV on yield at constant temperature of 520K, H₂/HC of 3.236 and pressure of 2.4MPa

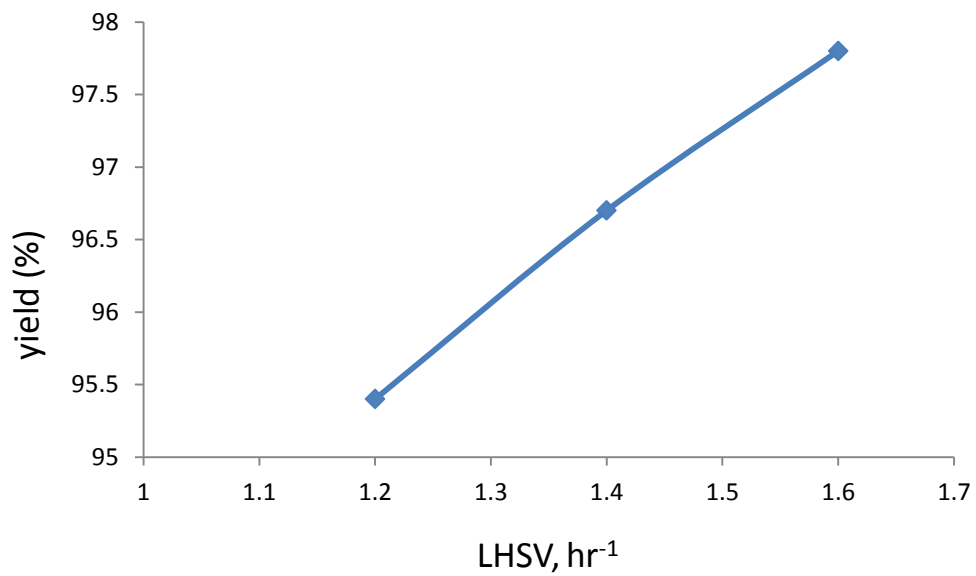


Figure 16: Effect of LHSV on yield at constant temperature of 523K, H₂/HC of 3.236 and pressure of 2.4MPa

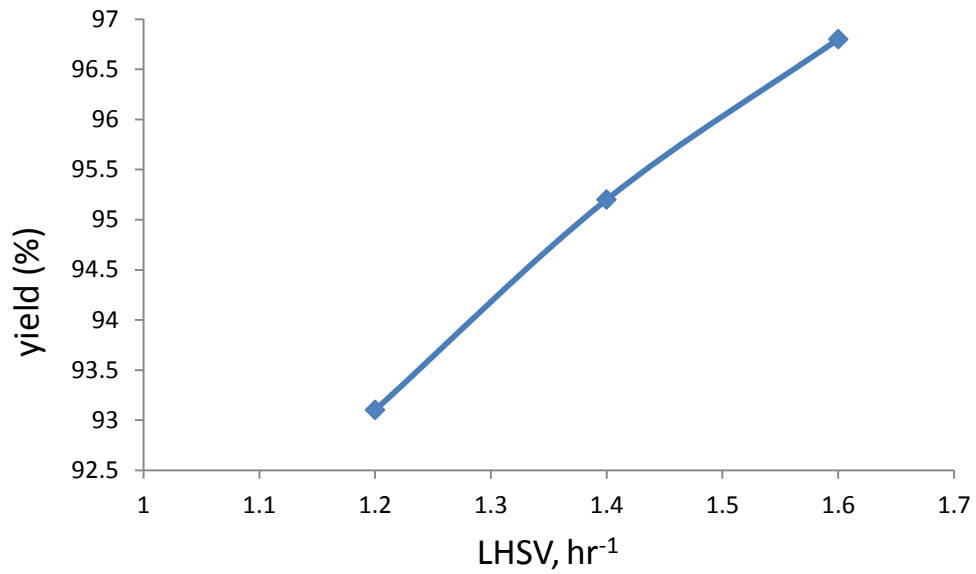


Figure 17: Effect of LHSV on yield at constant temperature of 526K, H₂/HC of 3.236 and pressure of 2.4MPa

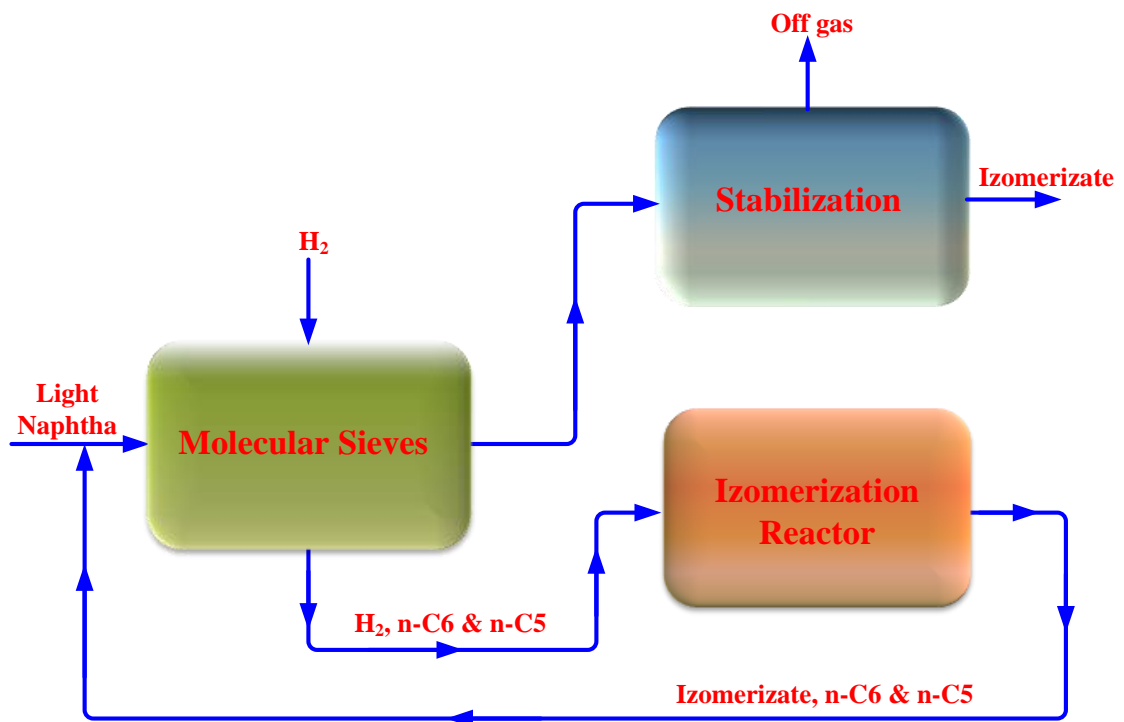


Figure 18: Block diagram of the proposed new isomerization process (named as AJAM process) in this study

Appendix A: Supporting information

Table A1: Lower and upper bounds for all listed inequality constraints of the applied model

Variable	Upper bounds	Lower bounds
E1 – E36	1E50	10
A1 – A36	1E50	10
n	3	0
m	2.5	0
o	10	0
α	10	0
γ	10	0

Table A2: Initial values for all listed inequality constraints of the applied model

Variable	Initial value
Temperature (T)	524.14 (K)
Concentration of normal hexane (C_{nC4})	0.009157242 (mol/m ³)
Concentration of normal pentane (C_{nC5})	0.058854476 (mol/m ³)
Concentration of normal hexane (C_{nC6})	0.029798934 (mol/m ³)
Concentration of normal heptane (C_{nC7})	0.002546383 (mol/m ³)
Concentration of iso-butane (C_{iC4})	6.68367E-4 (mol/m ³)
Concentration of iso pentane (C_{iC5})	0.04853589 (mol/m ³)
Concentration of di-methyl butane ($C_{2,2DMB}$)	0.0011211892 (mol/m ³)
Concentration of di-methyl butane ($C_{2,3DMB}$)	0.003171765 (mol/m ³)
Concentration of methyl pentane (C_{2MP})	0.01907564 (mol/m ³)
Concentration of methyl pentane (C_{3MP})	0.015434657 (mol/m ³)
Concentration of iso -heptane (C_{iC7})	0.0062734256 (mol/m ³)
Concentration of methyl cyclo pentane (C_{MCP})	0.005840283 (mol/m ³)
Concentration cyclo hexane (C_{CH})	0.003946619 (mol/m ³)
Concentration of benzene (C_B)	9.6205925E-4 (mol/m ³)
Concentration of cyclo pentane (Ccp)	0.0025210315 (mol/m ³)
Concentration of hydrogen (C_{H2})	0.50420004 (mol/m ³)
Concentration of gases (C_G)	0.0 (mol/m ³)